

1 **VERITAS Observations of the TeV Binary LS I +61° 303 During**
2 **2008-2010**

3 V. A. Acciari¹, E. Aliu², T. Arlen³, T. Aune⁴, M. Beilicke⁵, W. Benbow¹, S. M. Bradbury⁶,
4 J. H. Buckley⁵, V. Bugaev⁵, K. Byrum⁷, A. Cannon⁸, A. Cesarini⁹, L. Ciupik¹⁰,
5 E. Collins-Hughes⁸, M. P. Connolly⁹, W. Cui¹¹, R. Dickherber⁵, C. Duke¹², M. Errando²,
6 A. Falcone¹³, J. P. Finley¹¹, G. Finnegan¹⁴, L. Fortson¹⁵, A. Furniss⁴, N. Galante¹,
7 D. Gall¹¹, G. H. Gillanders⁹, S. Godambe¹⁴, S. Griffin¹⁶, J. Grube¹⁰, R. Guenette¹⁶,
8 G. Gyuk¹⁰, D. Hanna¹⁶, J. Holder^{17,*}, G. Hughes¹⁸, C. M. Hui¹⁴, T. B. Humensky¹⁹,
9 P. Kaaret²⁰, N. Karlsson¹⁵, M. Kertzman²¹, D. Kieda¹⁴, H. Krawczynski⁵, F. Krennrich²²,
10 M. J. Lang⁹, S. LeBohec¹⁴, G. Maier¹⁸, P. Majumdar³, S. McArthur⁵, A. McCann¹⁶,
11 P. Moriarty²³, R. Mukherjee², R. A. Ong³, M. Orr²², A. N. Otte⁴, N. Park¹⁹, J. S. Perkins¹,
12 M. Pohl^{18,24}, H. Prokoph¹⁸, J. Quinn⁸, K. Ragan¹⁶, L. C. Reyes¹⁹, P. T. Reynolds²⁵,
13 E. Roache¹, H. J. Rose⁶, J. Ruppel²⁴, D. B. Saxon¹⁷, M. Schroedter²², G. H. Sembroski¹¹,
14 G. Demet Senturk²⁶, A. W. Smith^{7,27*}, D. Staszak¹⁶, G. Tešić¹⁶, M. Theiling¹,
15 S. Thibadeau⁵, K. Tsurusaki²⁰, A. Varlotta¹¹, V. V. Vassiliev³, S. Vincent¹⁴, M. Vivier¹⁷,
16 S. P. Wakely¹⁹, J. E. Ward⁸, T. C. Weekes¹, A. Weinstein³, T. Weisgarber¹⁹,
17 D. A. Williams⁴, B. Zitzer¹¹

*Corresponding Authors: awsmith@hep.anl.gov, jholder@physics.udel.edu

¹Fred Lawrence Whipple Observatory, Harvard-Smithsonian Center for Astrophysics, Amado, AZ 85645, USA

²Department of Physics and Astronomy, Barnard College, Columbia University, NY 10027, USA

³Department of Physics and Astronomy, University of California, Los Angeles, CA 90095, USA

⁴Santa Cruz Institute for Particle Physics and Department of Physics, University of California, Santa Cruz, CA 95064, USA

⁵Department of Physics, Washington University, St. Louis, MO 63130, USA

⁶School of Physics and Astronomy, University of Leeds, Leeds, LS2 9JT, UK

⁷Argonne National Laboratory, 9700 S. Cass Avenue, Argonne, IL 60439, USA

⁸School of Physics, University College Dublin, Belfield, Dublin 4, Ireland

⁹School of Physics, National University of Ireland Galway, University Road, Galway, Ireland

¹⁰Astronomy Department, Adler Planetarium and Astronomy Museum, Chicago, IL 60605, USA

¹¹Department of Physics, Purdue University, West Lafayette, IN 47907, USA

¹²Department of Physics, Grinnell College, Grinnell, IA 50112-1690, USA

¹³Department of Astronomy and Astrophysics, 525 Davey Lab, Pennsylvania State University, University Park, PA 16802, USA

¹⁴Department of Physics and Astronomy, University of Utah, Salt Lake City, UT 84112, USA

¹⁵School of Physics and Astronomy, University of Minnesota, Minneapolis, MN 55455, USA

¹⁶Physics Department, McGill University, Montreal, QC H3A 2T8, Canada

¹⁷Department of Physics and Astronomy and the Bartol Research Institute, University of Delaware, Newark, DE 19716, USA

¹⁸DESY, Platanenallee 6, 15738 Zeuthen, Germany

¹⁹Enrico Fermi Institute, University of Chicago, Chicago, IL 60637, USA

²⁰Department of Physics and Astronomy, University of Iowa, Van Allen Hall, Iowa City, IA 52242, USA

²¹Department of Physics and Astronomy, DePauw University, Greencastle, IN 46135-0037, USA

²²Department of Physics and Astronomy, Iowa State University, Ames, IA 50011, USA

²³Department of Life and Physical Sciences, Galway-Mayo Institute of Technology, Dublin Road, Galway, Ireland

²⁴Institut für Physik und Astronomie, Universität Potsdam, 14476 Potsdam-Golm, Germany

²⁵Department of Applied Physics and Instrumentation, Cork Institute of Technology, Bishopstown, Cork,

18 **ABSTRACT**

19 We present the results of observations of the TeV binary LS I +61° 303 with the VERITAS telescope array between 2008 and 2010, at energies above 300 GeV. In the past, both ground-based gamma-ray telescopes VERITAS and MAGIC have reported detections of TeV emission near the apastron phases of the binary orbit. The observations presented here show no strong evidence for TeV emission during these orbital phases; however, during observations taken in late 2010, significant emission was detected from the source close to the phase of superior conjunction (much closer to periastron passage) at a 5.6 standard deviation (5.6σ) post-trials significance. In total, between October 2008 and December 2010 a total exposure of 64.5 hours was accumulated with VERITAS on LS I +61° 303, resulting in an excess at the 3.3σ significance level for constant emission over the entire integrated dataset. The flux upper limits derived for emission during the previously reliably active TeV phases (i.e. close to apastron) are less than 5% of the Crab Nebula flux in the same energy range. This result stands in apparent contrast to previous observations by both MAGIC and VERITAS which detected the source during these phases at 10% of the Crab Nebula flux. During the two year span of observations, a large amount of X-ray data were also accrued on LS I +61° 303 by the *Swift* X-ray Telescope (XRT) and the *Rossi X-ray Timing Explorer* (RXTE) Proportional Counter Array (PCA). We find no evidence for a correlation between emission in the X-ray and TeV regimes during 20 directly overlapping observations. We also comment on data obtained contemporaneously by the *Fermi* Large Area Telescope (LAT).

20 *Subject headings:*

21 **1. Introduction**

22 The high-mass X-ray binary LS I +61° 303 is one of only three such systems firmly identified as a source of TeV gamma rays. Despite many years of observations across the electromagnetic spectrum, the system remains, in some respects, poorly characterized. Known to

Ireland

²⁶Columbia Astrophysics Laboratory, Columbia University, New York, NY 10027, USA

²⁷Department of Physics and Astronomy, Northwestern University, Evanston, IL, 60208, USA

25 be the pairing of a massive B0 Ve star and a compact object of unknown nature (Hutchings
 26 and Crampton 1981, Casares 2005), LS I +61° 303 has been known historically for its ener-
 27 getic outbursts at radio, X-ray, GeV, and TeV wavelengths (Gregory et al 2002, Greiner and
 28 Rau 2001, Harrison et al. 2000, Abdo et al. 2009, Albert et al. 2008, Acciari et al. 2008), all
 29 of these showing correlation with the 26.5 day orbital cycle of the compact object in its path
 30 around the Be star. According to the most recent radial velocity measurements, the orbit
 31 is elliptical ($e = 0.537 \pm 0.034$), with periastron passage determined to occur around phase
 32 $\phi = 0.275$, apastron passage at $\phi = 0.775$, superior conjunction at $\phi = 0.081$ and inferior
 33 conjunction at $\phi = 0.313$ (Aragona et al. 2009). The non-thermal behavior of the source
 34 is well studied, yet poorly understood. The radio emission presents a well-defined periodic-
 35 ity with strong flares occurring periodically near apastron passage, along with an additional
 36 modulation on a 4.6 year timescale (Gregory 2002). The detection of extended structures in
 37 radio observations originally identified LS I +61° 303 as a potential microquasar, with high
 38 energy emission produced in jets driven by accretion onto the compact object, presumably
 39 a black hole (Massi et al 2001). High-resolution VLBA observations indicate that the radio
 40 structures are not persistent, however, and can be more easily explained by the interaction
 41 between a pulsar wind and the wind of the stellar companion (Dhawan et al. 2006, Albert
 42 et al. 2008), although alternative interpretations are still possible (Romero et al. 2007,
 43 Massi and Zimmerman 2010). The full range of arguments in favor of LS I +61° 303 as a
 44 non-accreting pulsar system have been summarized by Torres (2010a).

45 The X-ray behavior is well studied (see Smith et al. (2009) for a review), most compre-
 46 hensively in Torres et al. (2010b), in which the authors present an analysis of RXTE-PCA
 47 observations taken over four years, covering 35 full orbital cycles. They show that, while
 48 the X-ray emission from the source is indeed periodic, there is variability of the orbital pro-
 49 files on multiple timescales, from individual orbits up to years. Additionally, intense X-ray
 50 flares have been observed (Smith et al. 2009 and Torres et al. 2010b), during which the
 51 flux increases by up to a factor of five and variability on the timescale of a few seconds is
 52 observed. It is noted, however, that, due to the relatively large RXTE-PCA field-of-view
 53 ($\sim 1^\circ$ FWHM), the possibility that these flares are due to an unrelated source in the same
 54 field cannot be ruled out.

55 High-energy (HE; 30 MeV-30 GeV) gamma-ray emission, spatially coincident with
 56 LS I +61° 303, although with large positional errors, was first detected by COS-B (Hermsen
 57 et al. 1977) and, subsequently, by EGRET (Tavani et al. 1998). The detection of a variable
 58 very high energy (VHE; 30 GeV-30 TeV) gamma-ray source at the location of LS I +61° 303
 59 with MAGIC (Albert et al. 2006), later confirmed by VERITAS (Acciari et al. 2008), com-
 60 pleted the identification of this source as a gamma-ray binary. The TeV emission reported
 61 by both experiments for observations made prior to 2008 is spread over approximately one

62 quarter of the orbit, with a peak around apastron (orbital phase $\phi = 0.775$). *Fermi*-LAT
 63 observations provide the definitive HE detection and have revealed a number of interest-
 64 ing features (Abdo et al. 2009). The HE emission reported in the detection paper (based
 65 on observations from August 2008 until March 2009) is modulated at the orbital period
 66 (peaking slightly after periastron ($\phi = 0.225$)), although recent results from the LAT show
 67 different behavior (see Summary and Discussion). The overall Fermi spectrum shows a sharp
 68 exponential cutoff at 6 GeV.

69 The existence of orbital modulation in the gamma-ray flux is often explained by the
 70 varying efficiency of the inverse-Compton process around the orbit, although we note that
 71 many alternative explanations exist (see e.g. Sierpowska-Bartosik and Torres (2009) for a
 72 review). In this scenario, inverse-Compton gamma-ray production along our line of sight is
 73 most efficient at superior conjunction ($\phi = 0.081$), where stellar photons interact head-on with
 74 energetic leptons produced either directly in the pulsar wind or in the pulsar wind/stellar
 75 wind shock interaction region. The density of stellar photons may also play a role in the
 76 efficiency of gamma-ray production, with the highest density occurring at periastron. The
 77 TeV flux is further modulated by photon-photon absorption around the orbit, which peaks
 78 near superior conjunction and may dominate over the modulation effects due to production
 79 efficiency at energies above ~ 30 GeV. Orbital modulation of the GeV and TeV flux, with
 80 large differences between the lightcurves observed in each energy band, is therefore not
 81 unexpected. Other effects, for example Doppler boosting of the emission (Dubus et al.
 82 2010), clumps in the wind of the Be star (Araudo 2009), tidal disruption of the accretion
 83 disk (Romero et al. 2007) or cascading of high-energy photons to lower energies may also
 84 play a role, and provide a better fit of the models to the observations. However, it should be
 85 noted that the orbital inclination of the system is poorly constrained, and this complicates
 86 the modeling of emission from this system.

87 Substantial effort has been invested in constructing multiwavelength datasets on LS I +61° 303.
 88 Preliminary studies including TeV data (Acciari et al. 2009 and Albert et al. 2008) com-
 89 bined long-term (multi-orbit) observations at both X-ray and TeV wavelengths. Acciari et
 90 al. (2009) did not detect any correlation between emission at X-ray and TeV wavelengths
 91 with observations taken by VERITAS, *Swift*-XRT, and RXTE-PCA. However, the multi-
 92 wavelength observations used were not strictly overlapping, which is problematic given the
 93 observed fast (several seconds) variability in the X-ray regime detailed in Smith et al. (2009).
 94 Further X-ray/TeV observations reported in Anderhub et al. (2009) detect a correlation be-
 95 tween X-ray and TeV emission during a TeV outburst over a single orbital cycle. While the
 96 authors show a correlation (with a 0.5% probability of being produced from independent
 97 datasets), the longer-scale correlation behavior of the source outside of the observed flare is
 98 not well studied.

99 In this paper we summarize the results of VERITAS observations of LS I +61° 303
 100 between 2008 and 2010, including a comparison with strictly contemporaneous X-ray obser-
 101 vations. These are the first reported TeV observations since the launch of *Fermi* in June
 102 2008, and so they provide an opportunity to examine the broadband high-energy (100 MeV
 103 - 10 TeV) emission from the source using contemporaneous observations.

104 2. VERITAS Observations

105 The VERITAS array of imaging atmospheric Cherenkov telescopes (IACTs), located in
 106 southern Arizona (1250 m.a.s.l., 31°40' N, 110°57' W), is composed of four, 12m diameter,
 107 12m focal length telescopes, each with a Davies-Cotton tessellated mirror structure of 345
 108 mirror facets (total mirror area of 110 m²) (Ong et al. 2009) . Each telescope focuses
 109 Cherenkov light from particle showers onto a 499-pixel photomultiplier tube (PMT) camera.
 110 The pixels have an angular spacing of 0.15°, resulting in a camera field of view of 3.5°. During
 111 the summer months of 2009, one of the telescopes in the array was relocated, creating a more
 112 symmetric array layout and increasing the sensitivity of the observatory by 30% (Perkins et
 113 al. 2009). In its current configuration, VERITAS is able to detect a source with a flux of 1%
 114 of the steady Crab Nebula flux in under 30 hours. VERITAS has the capability to detect
 115 and measure gamma rays in the 100 GeV to 30 TeV energy regime with an energy resolution
 116 of 15-20% and an angular resolution of 0.1° (68% containment) on an event-by-event basis.

117 The VHE observations presented here were made with VERITAS between October 2008
 118 and December 2010, sampling eight separate orbital cycles of the binary system. The data
 119 comprise 64.5 live-time hours of observations taken with both the original (33.3 hours) and
 120 current (31.2 hours) array configurations. Data were taken using the complete four-telescope
 121 array; Cherenkov images which trigger two or more telescopes initiate a read-out of the 500
 122 MSpS Flash-ADC data acquisition on each PMT. The observations were made in “wobble”
 123 mode in which the source is offset from the center of the field-of-view of the cameras to
 124 maximize efficiency in obtaining both source and background measurements (Fomin et al.
 125 1994). After eliminating data taken under variable or poor sky conditions and applying im-
 126 age cleaning methods to reject images without sufficient signal for reconstruction, gamma-ray
 127 selection cuts were applied to the data. These selection cuts are based on the image morphol-
 128 ogy (*Mean Scaled Width* and *Length*), and the angular distance between the reconstructed
 129 position of the source in the camera plane and the *a priori* known source location. Cuts
 130 were optimized on simulated data for both the old and new array configurations; the analy-
 131 sis presented here was performed with cuts optimized for the detection of a moderately weak
 132 (5% Crab Nebula flux) source. The data on LS I+61°303 were taken over a relatively small

133 range of elevation angles (55° - 60°) under dark skies (little or no moonlight) resulting in an
 134 energy threshold for these observations of 300 GeV.

135 In the entire integrated dataset of 64.5 hours, 176 excess events above background were
 136 detected, corresponding to a 3.3σ statistical excess for steady emission, which does not
 137 constitute a significant detection. In Tables 1-3 and Figures 1-3 the results of the three
 138 years' observations are shown. For observations (both nightly, and binned by orbital phase)
 139 which did not exhibit a pre-trials excess above 3σ , 99% confidence level flux upper limits
 140 are calculated using the Helene method (Helene 1983). For nightly observations, these limits
 141 are typically on the order of $3\text{-}10 \times 10^{-12}$ photons $\text{cm}^{-2}\text{s}^{-1}$ above 300 GeV or 3-8% of the
 142 steady Crab Nebula flux. When binned by orbital phase, the limits extend down to 2-6
 143 $\times 10^{-12}$ photons $\text{cm}^{-2}\text{s}^{-1}$ above 300 GeV or 2-5% of the Crab Nebula. Particularly striking
 144 is the distinct lack of strong TeV emission during the apastron phases of $\phi = 0.5\text{-}0.8$ as these
 145 are the orbital phases during which both MAGIC and VERITAS have previously detected
 146 strong (10-20% Crab Nebula) emission.

147 Unexpectedly, in late 2010, gamma-ray emission from the source was detected over a
 148 region of the binary orbit previously undetected by TeV instruments (Ong, 2010). From
 149 September 17 to November 7 2010 (MJD 55455-55507), a total of 13.9 hours on LS I +61°
 150 303 were accumulated resulting in the detection of 129 excess events above background. This
 151 constitutes a detection at the 5.6σ post-trials significance level (5.7σ pre-trials significance
 152 with two trials for two sets of analysis cuts: standard analysis cuts and an analysis tailored
 153 for harder spectrum sources). During phases 0.0-0.1 (close to superior conjunction at phase
 154 0.081) the source was observed for a total of 4.2 hours. During this time a total of 66
 155 excess events were recorded, corresponding to a 4.8σ post-trials (5.4σ pre-trials) significance
 156 (accounting for twenty trials accumulated by analyzing the data in ten orbital phase bins
 157 with two sets of analysis cuts). Since this detection consists of too few events to construct
 158 a differential energy spectrum with comparable statistics to those previously published, we
 159 assume a spectral index of $\Gamma = 2.6$ (Acciari et al. 2008) in order to produce absolute fluxes.
 160 The source flux was measured as $6.86 \pm 1.45 \times 10^{-12}$ photons $\text{cm}^{-2}\text{s}^{-1}$ above 300 GeV, or
 161 approximately 5% of the Crab Nebula flux in the same energy range. The source presented
 162 the highest observed flux on October 8, 2010 (MJD 55477, $\phi = 0.07$) with 57 excess events
 163 detected in 2.8 hours of observations, corresponding to a 5.2σ post-trials (5.7σ pre-trials)
 164 significance, accounting for twenty trials accumulated by analyzing ten individual nights with
 165 two sets of analysis cuts to search for the maximal flux. During these observations the source
 166 flux was measured as $9.23 \pm 1.9 \times 10^{-12}$ photons $\text{cm}^{-2}\text{s}^{-1}$ above 300 GeV or approximately
 167 7% of the Crab Nebula flux.

168 It should be noted that after appropriate statistical trials are taken into account (for

169 binning on nightly and orbital timescales) the detection during phase 0.0-0.1 and on 10/08/10
 170 stand as the only statistically significant detections published by any TeV instrument since
 171 2007. The fact that these detections were made over a region of the orbit not previously
 172 suspected to be an active TeV phase is of particular interest.

173 3. X-ray Observations

174 The RXTE-PCA (Swank 1994) and *Swift*-XRT (see Gehrels et al. (2004) and Bur-
 175 rows et al. (2005)) data presented here were both obtained from the public data archive
 176 at <http://heasarc.gsfc.nasa.gov/> and analyzed using the HEASOFT (v6.9) package
 177 (Blackburn 1995). For RXTE-PCA analysis, standard data quality selection and screening
 178 (using the “rex” script in FTOOLS) was performed. All available data were extracted using
 179 only the top layer of Proportional Counting Unit #2 in each observation. The XSPEC 12.6
 180 software package (Arnaud 1996) was used to fit spectra with a simple absorbed power-law,
 181 assuming a fixed absorbing hydrogen column density (N_H) of $0.75 \times 10^{22} \text{ cm}^{-2}$ (Kalberla et
 182 al. 2005) between 3-10 keV and to extract fluxes in the 2-10 keV range. Fluxes were then de-
 183 absorbed using the Wisconsin photoelectric cross sections (Morrison and McCammon 1983),
 184 or the “wabs” model within XSPEC. Also, given that the PCA instrument on RXTE is
 185 known to give larger fluxes (on the order of 20%) on the same source as other more precise
 186 instruments (Tomsick et al. 1999), all the PCA fluxes quoted here have been reduced by a
 187 factor of 1.18 in order to provide a more accurate comparison to the *Swift*-XRT analysis.

188 For the *Swift*-XRT analysis, all data shown here were accumulated in “photon counting
 189 mode” and analyzed using the most recent *Swift*-XRT analysis tools with the HEASOFT
 190 6.2 package. The data were screened with standard filtering criteria and reduced using the
 191 *xrtpipeline* task. Background and source spectra were accumulated from each individual
 192 observation using circular regions of radius 60” and 20”, respectively. XSPEC 12.6 was used
 193 to fit accrued spectra in the 0.3-10 keV range using a simple, absorbed power law with the
 194 galactic hydrogen column density fixed at $0.75 \times 10^{22} \text{ cm}^{-2}$. Flux values and associated 1σ
 195 statistical errors were then calculated by integrating the fitted spectra over the 2-10 keV
 196 range.

197 Flux values as seen by both instruments (Figures 1-3) show a high degree of variability
 198 with values of $2\text{-}25 \times 10^{-12} \text{ ergs cm}^{-2} \text{ s}^{-1}$, consistent with other observations of LS I +61°
 199 303 with RXTE-PCA and *Swift*-XRT (i.e. Acciari et al. 2009).

200 Since variability of the X-ray emission from LS I +61° 303 has been demonstrated on
 201 various timescales, we select only data in the two bands which were directly overlapping in

202 time, so as to provide an accurate test for any correlation with VHE emission. Additionally,
 203 all of the simultaneous X-ray observations were first checked to confirm that there was
 204 no evidence for X-ray variability within the observation. There are twenty simultaneous
 205 observations taken in both X-ray and TeV (grey shaded regions) in the datasets examined
 206 here; eight from RXTE-PCA observations and twelve from the *Swift*-XRT observations. As
 207 can be seen in Figure 4, while the X-ray flux varies significantly, none of the points correspond
 208 to a significant TeV detection. A test for correlation between the two datasets results in a
 209 Pearson product-moment correlation coefficient of -0.03 ± 0.23 ; which is consistent with two
 210 uncorrelated datasets.

211 We note that the TeV exposures are typically significantly longer than the corresponding
 212 X-ray observations. This is unavoidable, given the requirement that the TeV exposure
 213 be sufficient to achieve a useful sensitivity; however, it introduces the possibility that the
 214 (unmeasured) X-ray flux may have varied considerably within the TeV observation.

215 To test whether the correlation between X-ray and TeV emission presented in Anderhub
 216 et al. (2009) would have been measurable in the data presented here, we compared the
 217 Anderhub correlation fit between X-ray and TeV data points to our data. This fit, along
 218 with the Anderhub data points from which it was derived, are shown in Figure 4. Since the
 219 energy range of our X-ray observations was different than that presented in Anderhub et
 220 al. (2-10 keV versus 0.3-10 keV), we have converted the Anderhub fit to our energy range.
 221 This modification was derived by scaling the 0.3-10 keV flux range along a spectral fit with
 222 index of $\Gamma=1.6$ (consistent with spectral measurements of the source found in Anderhub et
 223 al. 2009). Using this method, we arrive at a line fit of: $F(2-10 \text{ keV}) [10^{-12} \text{ ergs cm}^{-2} \text{ s}^{-1}]$
 224 $= (7.8 \pm 0.6) + (0.45 \pm 0.1) \times N(E > 300 \text{ GeV}) [10^{-12} \text{ cm}^{-2} \text{ s}^{-1}]$. According to this relation,
 225 the highest observed X-ray flux of $14.7 \pm 0.7 \times 10^{-12} \text{ ergs cm}^{-2} \text{ s}^{-1}$ leads to an expected TeV
 226 flux above 300 GeV of $15.3_{-5.2}^{+7.1} \times 10^{-12} \text{ photons cm}^{-2} \text{ s}^{-1}$ or approximately 10% of the Crab
 227 Nebula flux. For the overlapping observation in question, VERITAS observed the source for
 228 a total of 56 minutes and measured a negative fluctuation of events relative to background
 229 corresponding to a 99% Helene flux upper limit of $3.3 \times 10^{-12} \text{ photons cm}^{-2} \text{ s}^{-1}$, a factor of
 230 4.6 lower than the predicted value.

231 We note that this flux prediction does not take into account the uncertainty in what
 232 VERITAS would have actually measured in the observation time quoted. However, even
 233 under conservative estimates of VERITAS sensitivity (5σ detection of a 5% Crab-type source
 234 in ~ 1 hour), a source on the level predicted by the Anderhub correlation used here would
 235 likely have yielded strong evidence for a signal detection in the given observation livetime.

4. Contemporaneous *Fermi*-LAT GeV Observations

237 We performed aperture photometry on the *Fermi*-LAT dataset covering LS I +61°
 238 303 for the periods during which VERITAS accrued observations from 2008-2010. Using the
 239 publicly available Fermi analysis tools and an aperture radius of 2.4° (found to be optimal for
 240 this source in Abdo et al. 2009), we extracted the 100 MeV-300 GeV counts from the source
 241 in 26.5 day bins, and we used the *gtexposure* tools to calculate the exposure for each bin.
 242 Figure 5 shows the result of this analysis (without any background subtraction performed)
 243 along with the time periods during which VERITAS observed the source highlighted in
 244 grey regions. During each of the VERITAS observation windows indicated in the figure,
 245 VERITAS observed the source for typically 1-2 hours per night. The periods during which
 246 VERITAS successfully detected LS I +61° 303 in late 2010 (last three shaded regions in
 247 Figure 5) do not correspond to significantly higher or lower GeV flux than the previously
 248 observed regions during which VERITAS did not detect the source.

5. Summary and Discussion

250 We have presented the results of TeV observations of the Galactic binary LS I +61° 303
 251 made with the VERITAS array from October 2008 until December 2010. These observations
 252 covered eight separate 26.5 day orbital cycles with coverage (though not uniform) of all orbital
 253 cycles. A comparison with previous observations of this source is useful. In Figure 6 all three
 254 years of observations presented in this paper, along with the previously obtained detections
 255 by both VERITAS and MAGIC (Acciari et al. 2008, Acciari et al. 2009, Albert et al. 2008)
 256 are shown. In this figure we plot only points from previous observations that had detections
 257 above 3σ along with the currently obtained flux upper limits and detection near periastron.
 258 The previously published fluxes quoted at a different energy threshold were converted to >300
 259 GeV fluxes using a spectral index of -2.5, consistent with published spectra of the source
 260 (Acciari et al. 2009). The data shown here do not indicate any significant evidence for
 261 TeV emission during the orbital phases previously detected by VERITAS and MAGIC (i.e.,
 262 near apastron passage), with flux upper limits derived which are ~ 2 -3 times lower than the
 263 previously detected emission. Instead, the source has been detected for the first time during
 264 orbital phases 0.0-0.1, close to superior conjunction (at $\phi = 0.081$). A further implication
 265 of these observations is that there is no direct evidence that the process responsible for the
 266 detected *Fermi*-LAT emission continues beyond the published 6 GeV cut-off: all published
 267 spectra show only non-contemporaneous data.

268 An important caveat to these points is that we cannot rule out the existence of near-
 269 apastron TeV emission during the 2008-2010 timeframe. As is the case with all TeV obser-

270 vations, the sampling of the VHE flux from LS I +61° 303 was unavoidably limited, with
 271 observations taking place separated by days and only for integrations lasting several hours.
 272 Furthermore, since the orbital period of LS I +61° 303 (~ 27 days) is very close to the lu-
 273 nar cycle; full-orbit observations of LS I +61° 303 with ground-based TeV telescopes are
 274 limited by their inability to observe during bright moon phases. The observations sampled
 275 only 8 orbits out of 27 covered by these two years, and observations in 2009-2010 focussed
 276 exclusively on orbital phases $\phi = 0.5 - 0.8$. This leaves open the possibility that the source
 277 was active at VHE in some of the unobserved orbits during apastron passage. Also, the
 278 possibility exists that the sampling provided by the VERITAS observations simply missed
 279 the significant TeV activity.

280 We have also presented both contemporaneous and directly overlapping X-ray observa-
 281 tions taken with *Swift*-XRT and RXTE-PCA. The 20 directly overlapping X-ray observations
 282 do not show any evidence for correlation with the TeV emission. This stands in contrast
 283 somewhat to the result of Anderhub et al. (2009), in which a correlation was detected be-
 284 tween X-ray and TeV emission. However, the result of Anderhub et al. (2009) was obtained
 285 during a TeV outburst covering 60% of a single orbit, and this paper makes no claim of
 286 longer-term correlation between the two emission bands. We see no evidence for such a
 287 correlation during the observations taken here, which were obtained over several different
 288 orbital cycles.

289 During the 2008-2010 period, the GeV flux was monitored by *Fermi*-LAT. Dubois et
 290 al. (2010) have shown that the most recent *Fermi*-LAT GeV observations showed a marked
 291 flux increase, of $\sim 40\%$, in March 2009, after which the previously clear orbital GeV flux
 292 modulation is no longer measurable. The result of Torres et al. (2010b) shows that, while
 293 the X-ray periodicity of the source is well defined, it is not entirely stable; the degree of
 294 modulation, and the phase of the peak of the emission varies from orbit-to-orbit and year-
 295 to-year. These results, compounded by the TeV measurements in this paper, indicate that
 296 the non-thermal emission from LS I +61° 303 is not as stable as its southern hemisphere
 297 counterpart, LS 5039.

298 Torres (2010a) has suggested that the GeV emission characteristics can be simply ex-
 299 plained by invoking a two-component model, where the observed flux is the result of mag-
 300 netospheric (pulsar) emission, plus a wind contribution produced either in the inter-wind
 301 region and/or the pulsar wind zone. The magnetospheric contribution would be steady, and
 302 exhibit a sharp spectral cut-off at ~ 6 GeV, while the wind contribution would be expected
 303 to vary naturally with orbital phase. If the rate of particle acceleration is the main factor
 304 determining the GeV and TeV fluxes, then the observations reported here do not seem to
 305 support this idea in its simplest form. Since the wind component is expected to be sensitive

306 to orbital modulation, and it provides the primary contribution to the TeV emission, the
307 GeV flux increase since March 2009 should naturally lead to a larger fraction of the flux
308 being modulated with the orbital period, and to increased TeV flux. The opposite of both
309 of these effects is observed. Other factors may affect this conclusion, however; for example,
310 increased inverse-Compton cooling may cause the spectrum to steepen, enhancing the GeV
311 flux and decreasing the TeV flux. The system may also have moved into a state where the
312 Compton process has saturated, and the output spectrum is largely independent of the input
313 photon flux, thus explaining the disappearance of orbital modulation.

314 How can this apparent long term variability be explained? The results of radio moni-
315 toring (Gregory 2002) show a definite modulation of the phase and peak flux density of the
316 radio outbursts with a period of 1667 ± 8 days. In Gregory and Neish (2002) this effect is
317 attributed to a model where a pulsar is embedded in a co-planar fashion within the equato-
318 rial disk of the Be star. The long term modulation then results from periodic enhancements
319 of the stellar wind density within the disk. If this is the case, and the HE-VHE emission
320 results from the same particle population as the radio emission, then perhaps the long term
321 variation in these bands is not unexpected. It certainly seems likely, given the contrast with
322 the stability of the orbital lightcurves of LS 5039 (Kishishita et al. 2009, Aharonian et al.
323 2006, Abdo et al. 2009), that variations in the circumstellar environment of the Be star play
324 an important role in determining the variability of the observed emission. Sensitive TeV
325 observations of LS I +61° 303 began only in September 2005, while *Fermi* was launched in
326 June 2008. Continued monitoring over the coming years from X-ray to TeV will allow us to
327 probe longer-term cycles, to study the cross-correlations in more detail and to characterize
328 the emission spectra more precisely.

329 This research is supported by grants from the U.S. Department of Energy, the U.S.
330 National Science Foundation, the Smithsonian Institution, by NSERC in Canada, by Science
331 Foundation Ireland (SFI 10/RFP/AST2748) and by STFC in the U.K.. We acknowledge
332 the excellent work of the technical support staff at the Fred Lawrence Whipple Observatory
333 and the collaborating institutions in the construction and operation of the instrument.

334 The submitted manuscript has been created by employees of UChicago Argonne, LLC,
335 Operator of Argonne National Laboratory (“Argonne”) in conjunction with the VERITAS
336 collaboration. Argonne, a U.S. Department of Energy Office of Science laboratory, is op-
337 erated under Contract No. DE-AC02-06CH11357. The U.S. Government retains for itself,
338 and others acting on its behalf, a paid-up nonexclusive, irrevocable worldwide license in said
339 article to reproduce, prepare derivative works, distribute copies to the public, and perform
340 publicly and display publicly, by or on behalf of the Government.

341 J. Holder acknowledges the support of the NASA Fermi Cycle 2 Guest Investigator
342 Program (grant number NNX09AR91G).

343 **REFERENCES**

- 344 Abdo, A.A. et al., 2009, ApJ, 701:L123-L128
345 Abdo, A.A. et al., 2010, ApJSupp., 188, 405A
346 Acciari, V. et al. 2008, ApJ, 679, 1427
347 Acciari, V. et al. 2009, ApJ, 700, 2
348 Aharonian, F.A. et al., 2006, A&A, 460, 743
349 Albert, J. et al. 2006, Science, 312, 1771
350 Albert, J. et al. 2008, 684, 1351
351 Anderhub, H., et al. 2009, ApJ, 706, L27
352 Aragona, C. et al., 2009 ApJ 698, 514,
353 Araudo, A.T. 2009, A&A 503, 673
354 Arnaud, K.A. 1996, Astronomical Data Analysis Software and Systems V, eds. G. Jacoby,
355 and J. Barnes, ASP Conf. Series, volume 101, p17
356 Blackburn, J.K. 1995, Astronomical Data Analysis Software and Systems IV, eds. R.A.
357 Shaw, H.E. Payne, and J.J. E. Hayes, ASP Conf Ser. ,Vol 77, p367
358 Burrows, D.N. et al. 2005, Space Sci. Rev., 120, 165
359 Casares, J. et al. 2005, MNRAS, 360, 1105.
360 Dhawan, V. et al. 2006, in Proc. of Microquasars and Beyond: From Binaries to Galaxies,
361 in Proceedings of Science, Como, IT. ed. Belloni, T , p 52
362 Dubus, G., Cerutti, B., and Henri, G., 2010, A&A 516, A18
363 Dubois, R. et al., 2010, in Proc. “1st Sant Cugat Forum on Astrophysics; ICREA Workshop
364 on the high-energy emission from pulsars and their systems”, Sant Cugat, Spain.
365 April 2010
366 Fomin, V.P. et al. 1994, Astroparticle Physics, 2, 137
367 Gehrels, N. et al., 2004, ApJ, 611, 1005
368 Gregory, P.C. 2002, ApJ, 525, 427
369 Gregory, P. C. and Neish C. 2002, ApJ, 580, 1133

- 370 Greiner, J. and Rau, A. 2001, *A&A*, 375, 145
371 Harrison, F.A. et al. 2000, *ApJ*, 528, 454
372 Helene, O. 1983, *Nuc. Inst. and Meth.*, 212, 319
373 Hermsen, W. et al. 1977, *Nature*, 269, 494
374 Hutchings, J.D. and Crampton, D. 1981, *PASP*, 93, 486
375 Kalberla, P. M. W. et al. 2005, *A&A*, 440, 775
376 Kishishita, T. et al. 2009, *ApJ*, 697, L1
377 Massi, M. et al. 2001, *A&A*, 376, 217
378 Massi, M. and Zimmerman, L., 2010, *A&A*, 515, 82
379 Morrison, R. and McCammon, D., 1983, *ApJ* 270, 119
380 Ong, R.A. et al., 2009, in *Proc 31st ICRC*, Lodz, Poland, arXiv:0912.5355
381 Ong, R.A. et al., 2010, *Astronomers Telegram #2948*
382 Perkins, J. A. et al. 2009 *Fermi Symposium*, eConf Proceedings C091122
383 Romero, G.E. et al. 2007, *A&A* 474, 1522
384 Sierpowska-Bartosik, A. and Torres, D., 2009, *ApJ*, 693, 1462
385 Smith, A., Falcone, A., Holder, J., Kaaret, P., Maier, G., and Pandel, D. 2009, *ApJ*, 693,
386 1621
387 Swank, J.H. 1994, in *Proceedings of 181st American Astronomical Society Meeting*, Phoenix,
388 AZ, 185, 6701
389 Tavani, M. et al., 1998, *ApJ*, 497, L89
390 Tomsick, J. A., Kaaret, P., Kroeger, R. A., Remillard, R.A., 1999, *ApJ*, 512, 892
391 Torres, D. et al., 2010a, in *Proc. “1st Sant Cugat Forum on Astrophysics; ICREA Workshop*
392 *on the high-energy emission from pulsars and their systems”*, Sant Cugat, Spain,
393 April, 2010, arXiv:1008.0483
394 Torres, D. et al., 2010b, *ApJ*, 719, L104

MJD (UTC)	Phase (ϕ)	Livetime min	Significance σ	Flux/99% U.L. > 300 GeV $10^{-12} \gamma \text{ cm}^{-2} \text{ s}^{-1}$
54760.3	0.03	113.6	2.2	<10.1
54761.4	0.07	89.6	1.7	<9.9
54762.3	0.1	90.2	0.6	<6.8
54763.4	0.15	18.1	-0.4	<10.3
54764.2	0.18	111.5	0.5	<4.4
54765.2	0.22	126.9	-1.4	<2.6
54766.2	0.26	90.4	0.2	<5.9
54767.3	0.31	36.1	0.2	<6.9
54768.3	0.35	90.7	0.4	<6.0
54769.3	0.37	109.7	-0.3	<2.9
54770.3	0.41	54.7	-0.9	<4.4
54771.3	0.44	72.8	1.0	<6.5
54772.3	0.48	72.9	1.7	<10.2
54774.3	0.56	90.7	2.7	<9.2
54775.3	0.59	54.1	-0.7	<4.4
54776.3	0.63	162.5	1.5	<4.4
54777.4	0.67	72.5	0.5	<7.2
54778.4	0.71	54.4	-0.8	<5.8
54779.4	0.75	36.5	-0.3	<7.8
54856.1	0.64	102.9	0.4	<6.1
54857.1	0.68	90.5	-1.8	<2.7
54861.1	0.83	95.2	1.1	<7.4
54862.1	0.87	104.0	0.9	<6.8
54863.1	0.91	76.1	1.4	<8.8

Table 1: VERITAS observations of LS I +61° 303 in the 2008-2009 observing season.

MJD (UTC)	Phase (ϕ)	Livetime min	Significance σ	Flux/99% U.L.> 300 GeV $10^{-12} \gamma \text{ cm}^{-2} \text{ s}^{-1}$
55119.3	0.58	128.5	1.6	<7.3
55120.3	0.62	107.1	-0.4	<5.5
55121.3	0.65	161.6	-2.5	<1.6
55122.3	0.69	107.9	0.9	<6.0
55123.3	0.73	18.2	-0.7	<9.4
55124.3	0.77	99.2	1.9	<7.9
55146.2	0.59	146.3	3.4	5.8 ± 1.9
55151.2	0.78	123.2	2.1	<10.0
55175.2	0.69	54.7	-0.7	<6.5
55176.2	0.73	54.6	-0.3	<7.3
55177.2	0.76	18.2	-0.8	<10.3

Table 2: The same as Table 1, but for the 2009-2010 observing season.

MJD (UTC)	Phase (ϕ)	Livetime min	Significance σ	Flux/99% U.L.> 300 GeV $10^{-12} \gamma \text{ cm}^{-2} \text{ s}^{-1}$
55455.4	0.26	55.4	1.7	<10.08
55457.4	0.33	18.0	1.4	<18.00
55476.4	0.05	91.7	1.3	<11.4
55477.3	0.09	162.6	5.7	9.23 ± 1.9
55480.3	0.2	54.2	2.3	<19.7
55481.3	0.24	107.9	2.0	<9.3
55482.3	0.28	108.3	-0.3	<4.2
55483.3	0.32	128.1	-0.04	<5.84
55505.3	0.14	36.5	2.7	<23.7
55506.2	0.18	73.3	0.9	<11.09

Table 3: The same as Table 1, but for the 2010-2011 observing season.

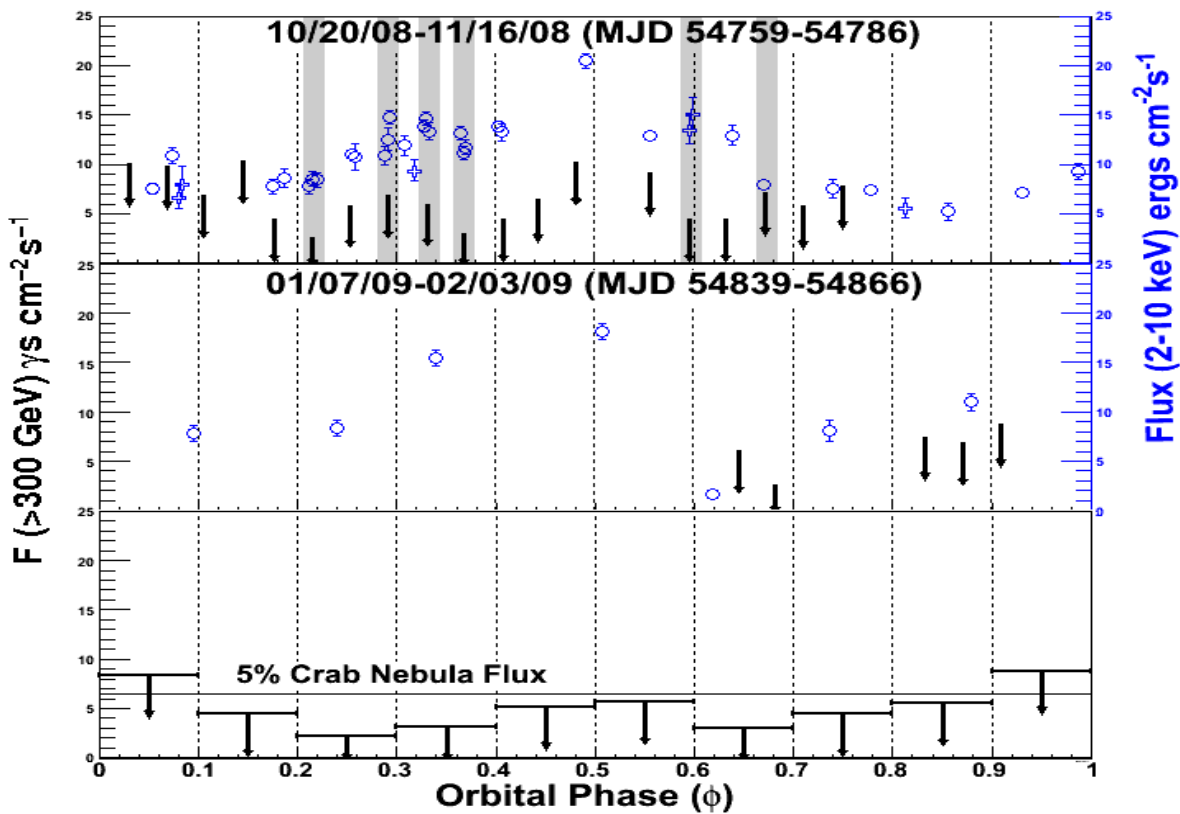


Fig. 1.— TeV flux upper limits from VERITAS (black points and arrows) compared to contemporaneous X-ray fluxes as measured by *Swift*-XRT (blue crosses) and RXTE-PCA (blue open circles). The bottom panel shows the integrated result from the two measured orbital cycles observed from October 2008 to February 2009. VERITAS flux measurements with less than 3σ pre-trials significance are shown as 99% confidence flux upper limits. The shaded regions indicate observations which had directly overlapping X-ray measurements by either RXTE or *Swift*.

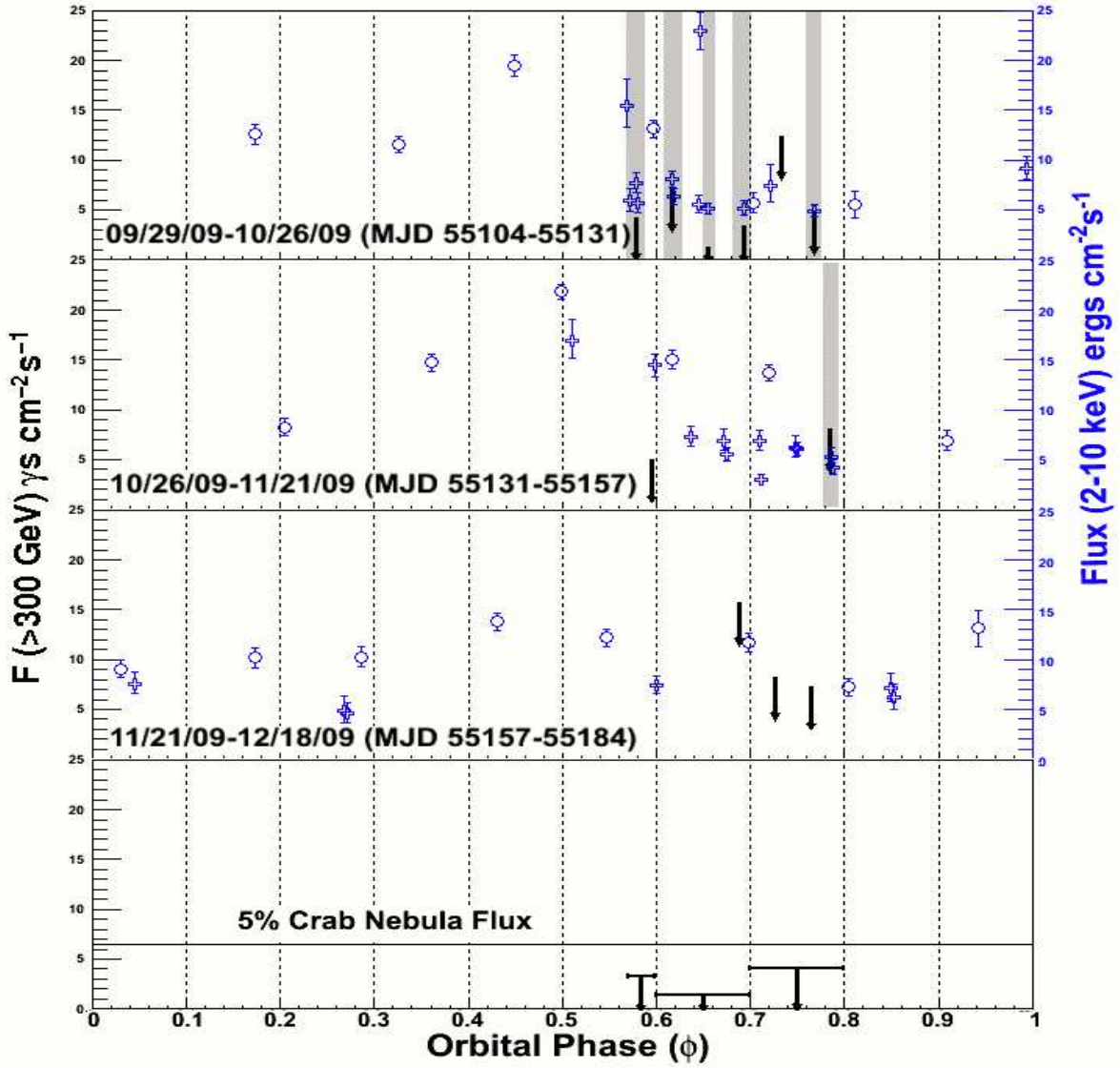


Fig. 2.— The same as Figure 1, but for the 2009-2010 observing season.

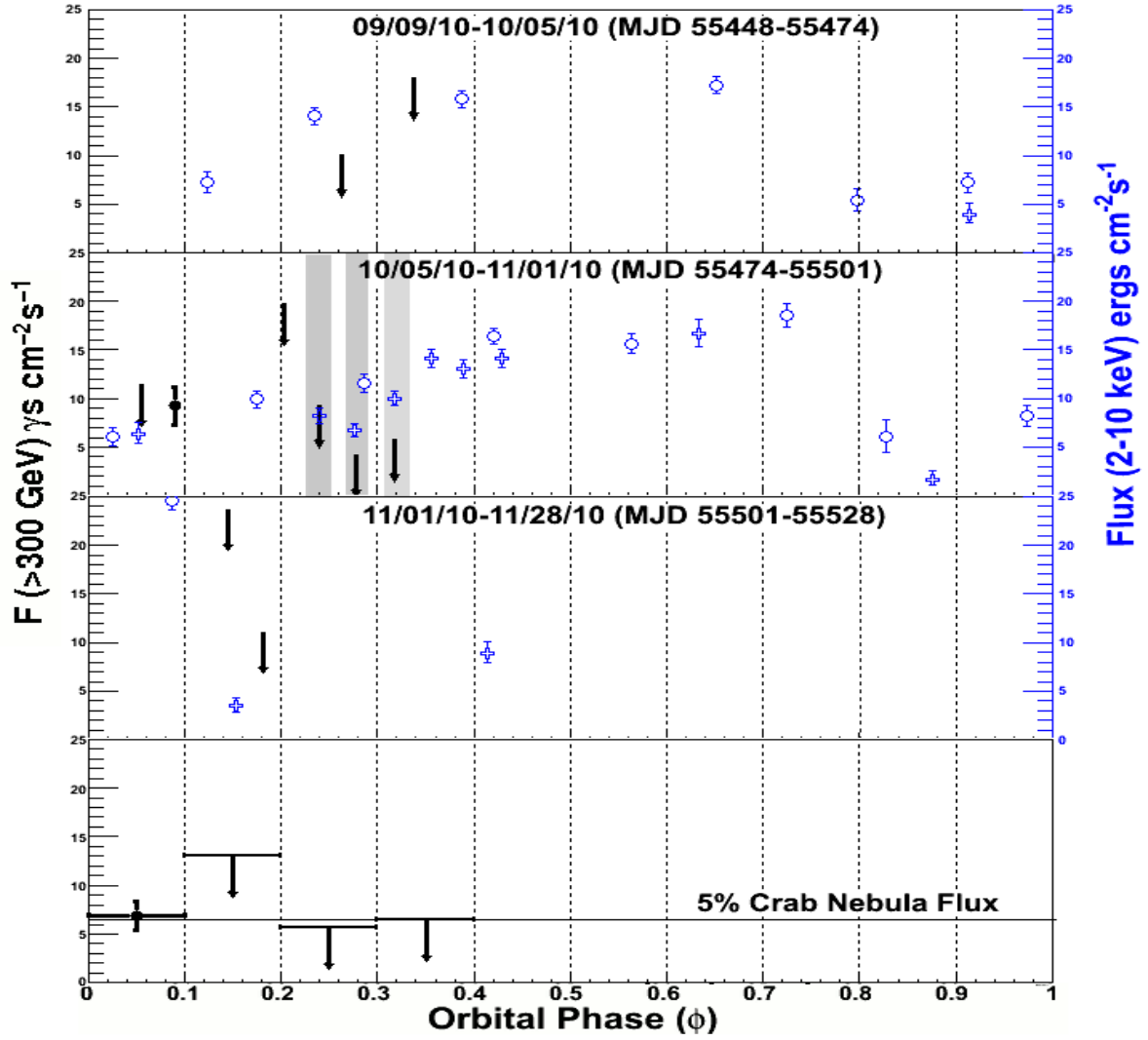


Fig. 3.— The same as Figure 1, but for the 2010-2011 observing season.

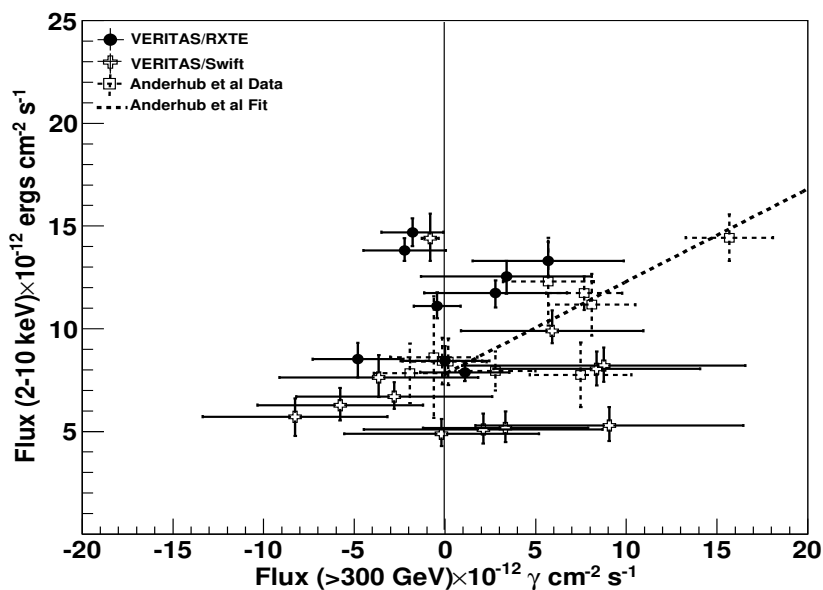


Fig. 4.— A comparison of the strictly simultaneously observed TeV and X-ray fluxes seen by VERITAS and *Swift*/RXTE, along with the data points and associated correlation fit from Anderhub et al. (2009).

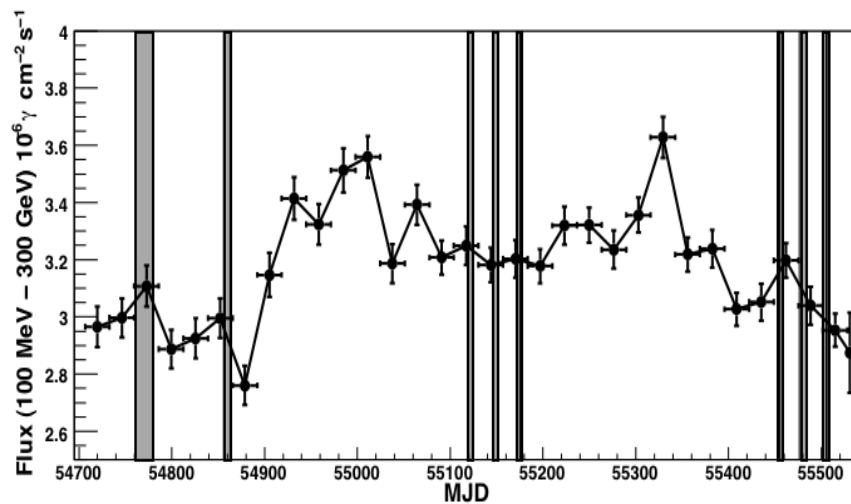


Fig. 5.— The GeV flux observed by *Fermi*-LAT from LS I +61° 303 (with no background subtraction performed). The grey shaded regions show the times during which VERITAS observed the source during 2008-2010.

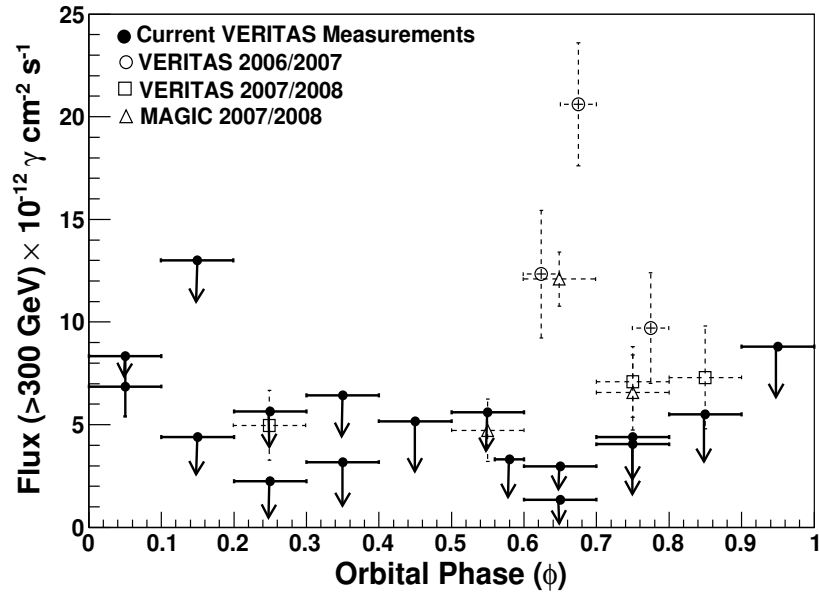


Fig. 6.— The observations presented in this paper (solid lines) along with previous observations (dashed lines) from Acciari et al (2008), Acciari et al (2009), and Albert et al. (2008). Only detections at a significance larger than 3σ are shown from previous observations.